International Journal of Mass Spectrometry 291 (2010) 33–40

Contents lists available at ScienceDirect

International Journal of Mass Spectrometry

journal homepage: www.elsevier.com/locate/ijms

Structural analysis and differentiation of reducing and nonreducing neutral model starch oligosaccharides by negative-ion electrospray ionization ion-trap mass spectrometry

Richard Čmelík*, Josef Chmelík

Institute of Analytical Chemistry of the ASCR, v. v. i., Veveří 97, 602 00 Brno, Czech Republic

ARTICLE INFO

Article history:
Received 27 February 2009
Received in revised form
24 December 2009
Accepted 4 January 2010
Available online 13 January 2010

Keywords:
Structural analysis
Oligosaccharides
Starch
Electrospray mass spectrometry
Negative-ion mode

ABSTRACT

Negative-ion electrospray tandem mass spectrometry with an ion-trap provided a sensitive tool for sequence determination of oligosaccharides derived from starch. Fragmentations of $[M-H]^-$ as well $[M+Cl]^-$ ions allow an unambiguous differentiation between α-(1 → 4) and α-(1 → 6) linkage based on the presence of diagnostic $[M-H-90]^-$ and $[M-H-78]^-$ ions. For nonreducing saccharides with terminal sucrose groups, the fragmentation starts with elimination of the fructose unit, followed by cross-ring cleavages of the remaining rings. The specific fragmentation features of reducing and nonreducing saccharides can be used for their differentiation.

1. Introduction

Starch is a naturally abundant reserve polysaccharide produced by photosynthesis in plants. It is found mainly in the seeds, fruits, tubers, and roots and varies widely in appearance according to source and growing period. It is composed of two components, amylose (15–25%) and amylopectin. Amylose essentially is a linear polymer of α-(1 → 4)-linked D-glucopyranosyl units with few (<0.1%) α-(1 → 6) linkages [1]. Amylopectin consists of α-(1 → 4) linked D-glucose chains and is relatively high branched with 5–6% α-(1 → 6)-bonds [2]. The length of amylose-like chains to branched structure may vary between 10 and 100 glucose units [3]. Related nonreducing oligosaccharides in plants are represented by raffinose-family oligosaccharides consisting of the repeating α-(1 → 6)-galactopyranosyl units and terminal sucrose moiety. Oligomers were found up to pentadecasaccharides. They have important functions such as cold and desiccation tolerance, and serve as storage and transport saccharides [4].

To understand relations between physical properties, chemical behavior and the functionality of starch it is important to characterize its structure. A structural analysis of saccharides requires the determination of included monosaccharides, their sequence, the type of linkages between monosaccharide units, branching and anomeric configuration. Although the development of physicochemical analytical methods improved the situation, analysis of oligosaccharides is still a difficult task. Mass spectrometry (MS) is a unique tool for the structural analysis of saccharides and offers precise results, analytical versatility and very high sensitivity. Previously, the "soft" mass spectrometric ionization techniques, such as fast atom bombardment (FAB), have gained attention as approaches to investigate oligosaccharides [5]. Over the past decades the FAB technique has been replaced by the more sensitive techniques of electrospray ionization (ESI) and matrix-assisted laser desorption/ionization (MALDI) [6,7].

With MS, saccharides can be studied in both positive-ion and negative-ion modes. Both modes can be applied to neutral oligosaccharides that can be generally detected as adduct molecule ions with alkali metal ions in the positive-ion mode and as deprotonated molecules (or their fragments) or adduct molecule ions with anions in the negative-ion mode [8–10]. Various anions can be added in order to increase the response of saccharides in the negative-ion mode [9,11]. MS structural analysis is based on MS^n experiments ($n \geq 2$). The key problem is to find diagnostic fragment ions that enable discrimination among alternative structures. Fragmentations of saccharides have different features in the positive-ion and negative-ion modes [7]. $[M+Na]^+$ ions provide MS^2 spectra containing both glycosidic and cross-ring fragments [12,13]. In the negative-ion mode, the predominant ion derived from saccharides

* Corresponding author. Tel.: +420 532 290 216; fax: +420 541 212 113.
E-mail address: cmelik@iach.cz (R. Čmelík).

1387-3806/$ – see front matter © 2010 Elsevier B.V. All rights reserved.
doi:10.1016/j.ijms.2010.01.001

Table 1
The list of oligosaccharides and their structures used in this work.

Maltotriose	α-D-Glc*p*-(1 → 4)-α-D-Glc*p*-(1 → 4)-D-Glc*p*
Maltose	α-D-Glc*p*-(1 → 4)-D-Glc*p*
Erlose	α-D-Glc*p*-(1 → 4)-α-D-Glc*p*-(1 ↔ 2)-β-D-Fru*f*
Isomaltotriose	α-D-Glc*p*-(1 → 6)-α-D-Glc*p*-(1 → 6)-D-Glc*p*
Isomaltose	α-D-Glc*p*-(1 → 6)-D-Glc*p*
Melibiose	α-D-Gal*p*-(1 → 6)-D-Glc*p*
Stachyose	α-D-Gal*p*-(1 → 6)-α-D-Gal*p*-(1 → 6)-α-D-Glc*p*-(1 ↔ 2)-β-D-Fru*f*
Panose	α-D-Glc*p*-(1 → 6)-α-D-Glc*p*-(1 → 4)Glc*p*
Sucrose	α-D-Glc*p*-(1 ↔ 2)-β-D-Fru*f*
Turanose	α-D-Glc*p*-(1 → 3)-D-Fru*f*
Palatinose	α-D-Glc*p*-(1 → 6)-D-Fru*f*

is $[M-H]^-$ but these ions frequently give rise to in-source fragments. Fragmentation of deprotonated molecules gives the ions diagnostic of the linkage type between adjacent units [5]. Chloride adducts provide comparable spectra [14,15]. Therefore, intact saccharides should be subjected to a two-step analysis. Firstly, positive-ion mass spectra provide information concerning the monosaccharide sequence of the sugar core and secondly, negative-ion mass spectra reveal, in addition, all linkage positions [8,16].

Discrimination between different glucose oligomers, including α-(1 → 4) and/or α-(1 → 6) linkages, was reported several times. The FAB [5] and ESI mass spectra [17] of deprotonated molecules of oligosaccharides provide important information for characterizing the glycosidic linkage type. Similarly, the fragmentation behavior of disaccharides in the negative-ion mode was characterized by liquid secondary ion MS and related to the fragmentation behavior of larger oligomers [18]. In other experiments collision-induced dissociation of ammonium [17], sodium [17,19,20], and lithium adducts [17,21], as well dilithiated species, $[M+2Li-H]^+$ [22], were used. Maltooligosaccharides in marine mucilage were investigated by the ESI-MS^2 technique [23].

In the studies cited, emphasis was placed on mass spectral description of isomeric disaccharides and higher oligosaccharides, focusing on one type of saccharide-derived ions, in particular in the positive-ion mode. Attention was paid on a heterogeneous series of target compounds involved several monomers and/or glycosidic linkages, as well as anomericity.

Here, we report the differentiation of isomers of oligosaccharides, especially α-(1 → 4) and α-(1 → 6) types of glycosidic linkages using an ESI ion-trap (IT) MS. This technique combines more gentle ionization of saccharides than MALDI [10] and has MS^n capability—a very efficient tool for elucidation of saccharide structure [12]. First, our approach is comprised of a comprehensive comparison of fragmentation behavior both of $[M+Na]^+$ and $[M-H]^-$ (or $[M+Cl]^-$) ions derived from model samples of oligosaccharides. Next, we investigated the samples without both the derivatization and the addition of ionic dopants. It represents a simple method for analysis of saccharides with structural features of starch.

2. Experimental

All oligosaccharides were obtained from Sigma (St. Louis, USA) and used without purification. The sample solutions were prepared in deionized water at a concentration of 10 μM.

The electrospray mass spectra were recorded with an Esquire LC ion-trap mass spectrometer (Bruker Daltonik GmbH, Bremen, Germany) equipped with an ESI source. Sample solutions were introduced into the ion source at a flow rate of 3 μL/min via a metal capillary held at high voltage (±3.5 kV). The other instrument conditions were as follows: drying gas temperature, 250 °C; drying gas flow, 5 L/min; nebulizer pressure, and 14 psi. Nitrogen was used as both nebulizing gas and drying gas. The nozzle-skimmer potential and octopole potential were modified and optimized before each experiment. Ions were scanned in the range of *m/z* 50–1500 at a scan speed of 13,000 Da/s, and 25 scans were averaged for each spectrum. The maximum number of ions allowed in the ion-trap was set at 5000 with a maximum acquisition time of 200 ms. For MS^2 experiments the precursor ion isolation width was set to 5 Da,

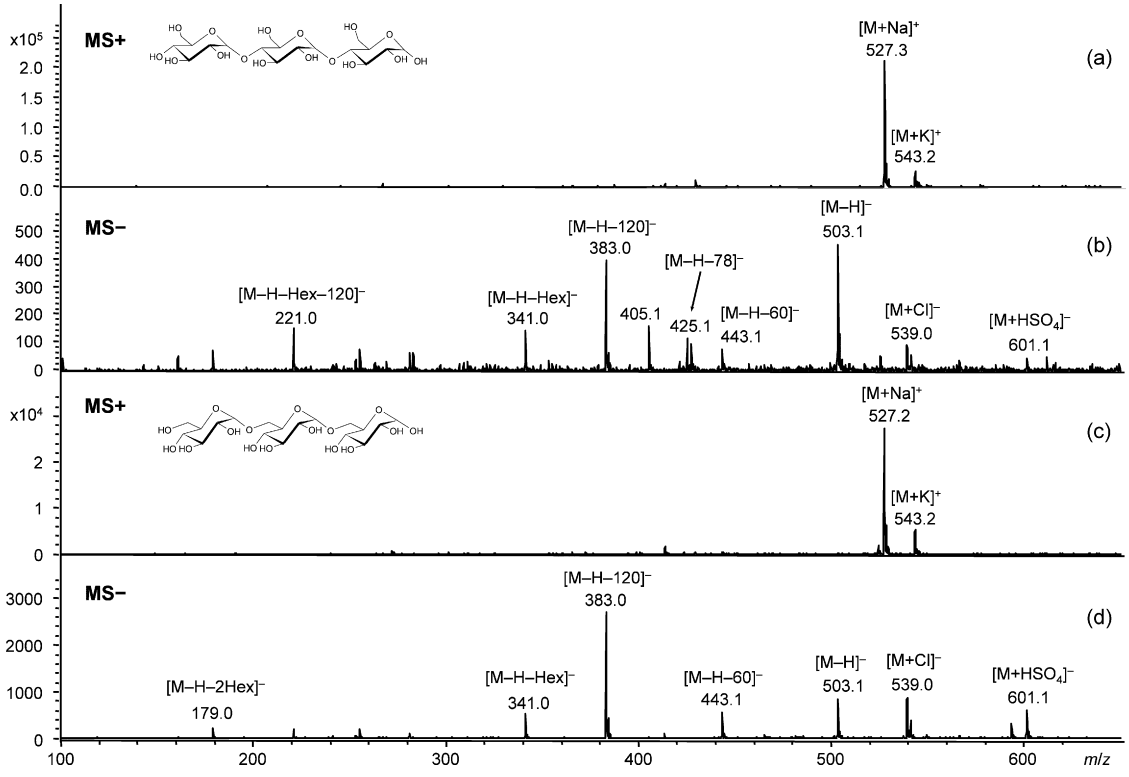

Fig. 1. Mass spectra of maltotriose (a and b) and isomaltotriose (c and d) in both positive- and negative-ion modes.

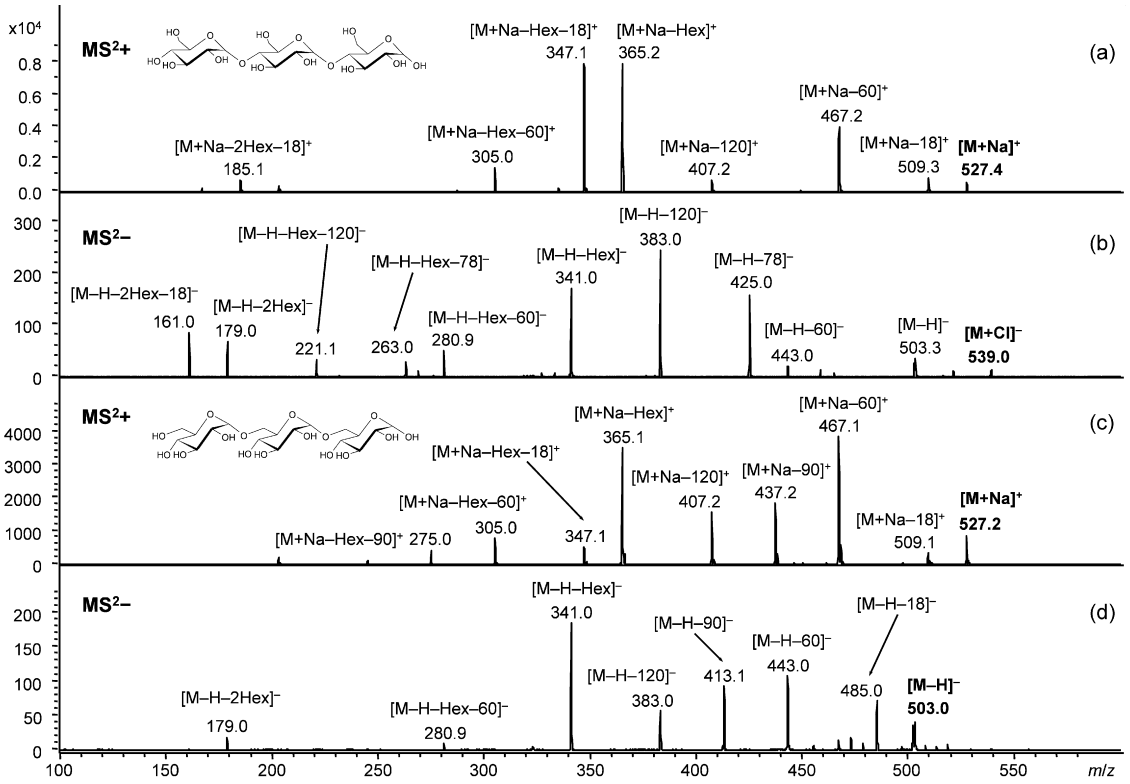

Fig. 2. Positive-ion ESI-MS^2 spectra of $[M+Na]^+$ ions from maltotriose (a) and isomaltotriose (c). Negative-ion ESI-MS^2 spectra of $[M+Cl]^-$ ion from maltotriose (b) and $[M-H]^-$ ion from isomaltotriose (d). Precursor ions are indicated in bold print.

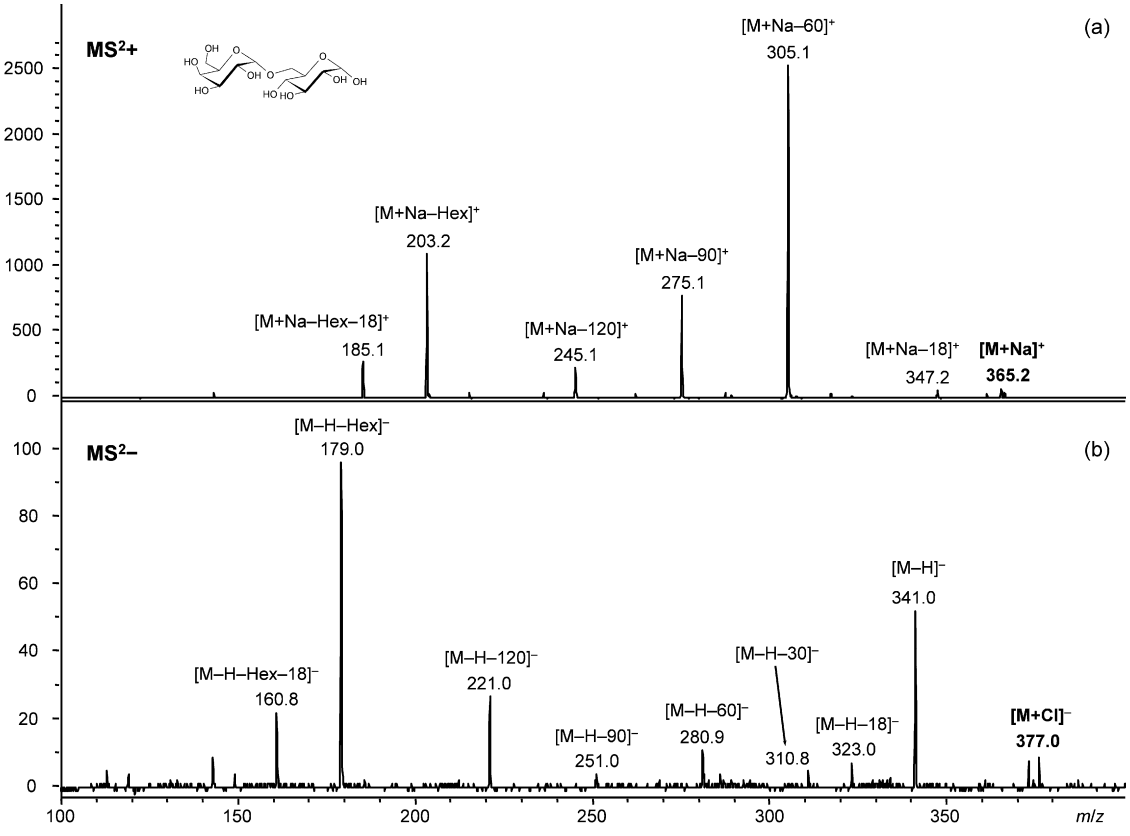

Fig. 3. ESI-MS^2 spectra of $[M+Na]^+$ (a) and $[M+Cl]^-$ (b) ions from melibiose.

and the fragmentation amplitudes were varied between 0.5 and 1.2 V to reduce the intensity of the precursor ion to 10% of its initial intensity. The fragmentation time was 40 ms, the low-mass cut-off was set at default 1/3 of the precursor m/z value. For the MS^3 experiment the isolation width was 5 Da and the fragmentation amplitude was 0.95 V.

3. Results and discussion

The set of eleven oligosaccharides (six disaccharides, four trisaccharides, and one tetrasaccharide), including five nonreducing (erlose, stachyose, sucrose, turanose and palatinose) was selected to be ionized and fragmented by ESI-IT-MS (see Table 1). The structural information was obtained from the relationship between the type of glycosidic linkage and the presence of specific fragment ions in the MS^2 spectra. Experiments started with maltotriose and isomaltotriose which were analyzed to determine the general fragmentation pattern. The main features of pattern were compared with those of the corresponding disaccharides (maltose and isomaltose) and melibiose. Fructosylated oligosaccharides (palatinose, turanose, sucrose) of different linkages, were investigated aimed at showing the influence of the linkage type on fragmentation pattern. The MS^2 spectra of various structures were compared. Additionally, the study was extended to tri- and tetra-saccharides, panose, erlose, and stachyose which contain the sucrose disaccharide unit. Mass spectra presented here were acquired in both negative- and positive-ion modes.

The number of the ionic species recorded in the negative-ion mode was rather high: deprotonated molecules $[M-H]^-$, their fragments $[M-H-X]^-$, a certain amount of deprotonated sodium adducts $[M+Na-2H]^-$ (e.g., for erlose), chloride $[M+Cl]^-$, and hydrogen sulfate $[M+HSO_4]^-$ adducts. An anion attachment is related to the sample contamination with traces of inorganic salts. (However, the purification of the sample is not essential due to the very similar product ion spectra of both $[M-H]^-$ and $[M+Cl]^-$). Both cross-ring and glycosidic fragments of the deprotonated molecules were found in the negative-ion mass spectra of the reducing saccharides [24]. On the contrary, positive-ion mass spectra were simpler with regard to the variety of the ion species. Sodiated molecules dominated, accompanied by the less abundant potassium adduct ions. The differences between the positive- and negative-ion modes in the cases of maltotriose and isomaltotriose are displayed in Fig. 1.

The MS^2 spectra obtained for maltotriose and isomaltotriose in both modes are depicted in Fig. 2. In the negative-ion mode, the abundant $[M-H]^-$ and $[M+Cl]^-$ ions were selected for the fragmentation. The molecular masses of the fragment ions of maltotriose (Fig. 2b) corresponded to $[M-H-60]^-$, $[M-H-78]^-$, $[M-H-120]^-$, and $[M-H-Hex]^-$ ions (the abbreviation Hex represents any hexose). The similar fragmentation pattern was observed for mass region m/z 179–365. In comparison, isomaltotriose fragmentation (Fig. 2d) yielded $[M-H-18]^-$, $[M-H-60]^-$, $[M-H-90]^-$, $[M-H-120]^-$, and $[M-H-Hex]^-$ ions. The most important differences obtained by the comparison of both MS^2 spectra were represented by the neutral loss of 90 Da for maltotriose and 78 Da for isomaltotriose. Generally, we determined that the fragment ion $[M-H-90]^-$ can be used as a useful diagnostic ion for α-(1 → 6) linkages and $[M-H-78]^-$ for α-(1 → 4) linkages. These conclusions were further supported with the MS^2 spectra of selected ions from melibiose (Fig. 3b), maltose, and isomaltose (see Table 2). Moreover, Fig. 3b shows that both deprotonated molecules and chloride adducts can be used for successful characterization of oligosaccharide structure. The MS^2 spectrum of the chloride adduct of melibiose showed the analogous fragment ions as those formed from the deprotonated molecules of isomaltotriose (cf. Fig. 2d). The presence of an ion at m/z 341 corresponded to the additional release of HCl from this adduct. Similar fragmentation behavior of chloride adducts was also observed for the other reducing saccharides (e.g., for panose in Fig. 4f).

Fragmentations of $[M+Na]^+$ ions were similar for all samples and contained cross-ring fragments $[M+Na-X]^+$ (where X corre-

Table 2
Comparison of fragment ions obtained from several oligosaccharides in positive- and negative-ion ESI-MS^2 spectra. The observed fragment ions were formed from $[M+Na]^+$ (indicated with *), $[M-H]^-$ (indicated with x), and $[M+Cl]^-$ (indicated with +), where M corresponds to molecule of saccharide.

Ion type	$[M+Na-Hex-X]^+$						$[M+Na-X]^+$							Bond type
X =	Hex	120	**90**	78	60	18	Hex	120	**90**	78	60	30	18	
Maltotriose	*				*	*	*	*			*		*	1–4
Maltose						*	*				*		*	1–4
Erlose[a]	*					*	*							1–4
Isomaltotriose							*	*	*		*		*	1–6
Isomaltose							*	*	*		*			1–6
Melibiose						*	*	*	*		*		*	1–6
Stachyose[a]	*				*	*	*							1–6
Panose	*				*	*	*	*			*		*	1–6, 1–4
Sucrose[a]						*	*							
Turanose[a]							*		*		*		*	
Palatinose[a]							*	*	*		*	*	*	

Ion type	$[M-H-Hex-X]^-$						$[M-H-X]^-$							Bond type
X =	Hex	120	**90**	**78**	60	18	Hex	120	**90**	**78**	60	30	18	
Maltotriose	+	+		**+**	+		+	+		**+**	+			1–4
Maltose						+	+	+		**+**	+			1–4
Erlose[a]	x	x		**x**	x	x	x							1–4
Isomaltotriose	x, +				x, +		x, +	x, +	**x, +**		x, +		x	1–6
Isomaltose						x, +	x, +	x, +	**x, +**		x, +	x	x, +	1–6
Melibiose						+	+	+	**+**		+	+	+	1–6
Stachyose[a]	x	x	**x**		x	x	x							1–6
Panose	x, +	x, +	**x, +**		x, +	x, +	x, +	+		**x, +**			x	1–6, 1–4
Sucrose[a]					x	x	x, +							
Turanose[a]						+	+		**+**					
Palatinose[a]					+	+	x, +	x, +	**x, +**		x, +	x	x, +	

Diagnostic fragments are in bold.
[a] Nonreducing oligosaccharides.

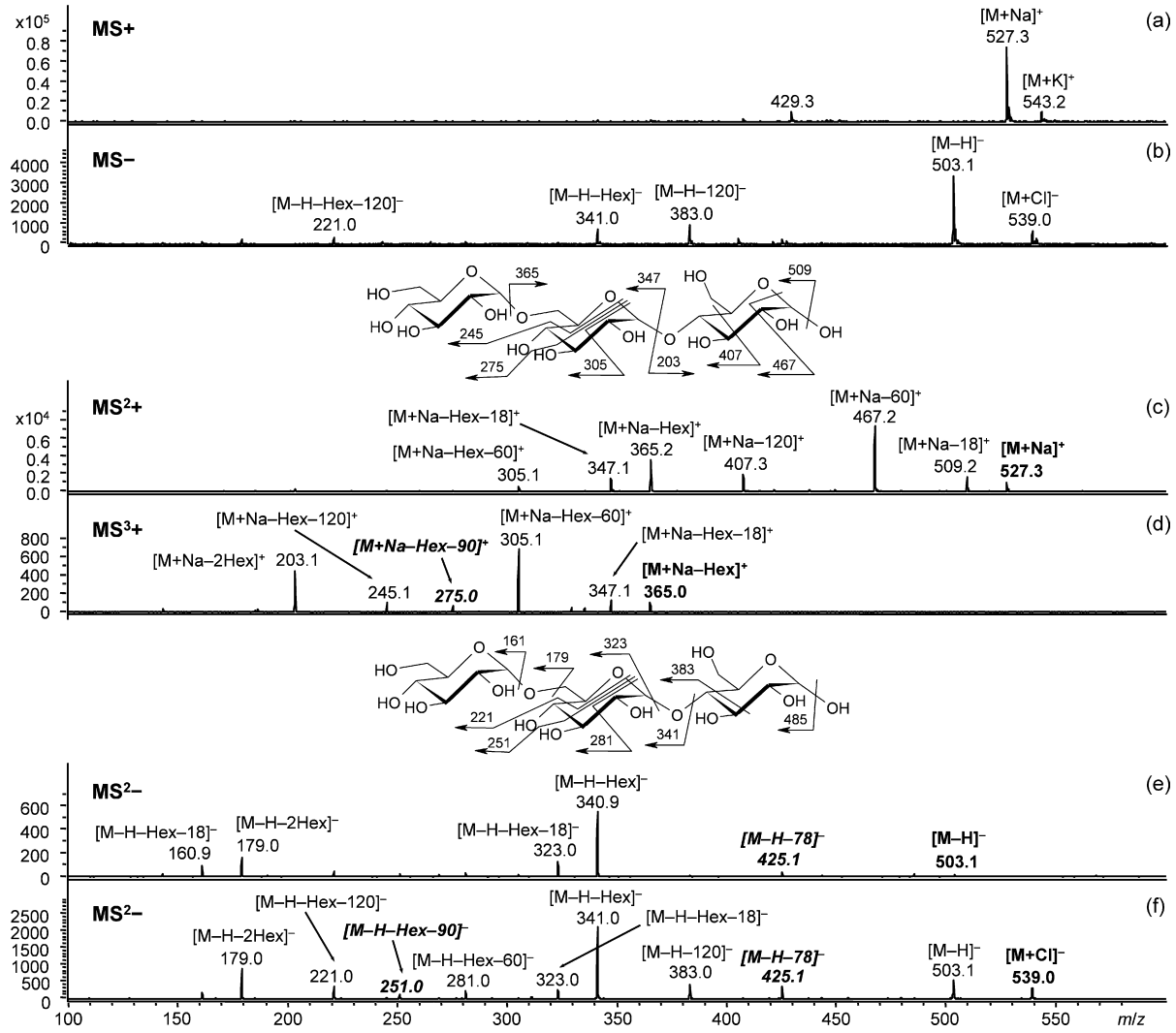

Fig. 4. Mass spectra of panose: positive- (a) and negative-ion (b) mass spectrum. MS^2 spectra of $[M+Na]^+$ (c), $[M-H]^-$ (e), and $[M+Cl]^-$ (f). MS^3 spectrum of $[M+Na-Hex]^+$ (d). Precursor ions are in bold, diagnostic fragment ions are in bold italics. Cleavages of panose molecule are indicated in the molecular structure above corresponding spectra.

sponded to 60 and 120) and ions derived from cleavage of glycosidic bond. The $[M+Na-90]^+$ ions were detected only in the cases of oligosaccharides containing α-(1 → 6) linkage, e.g., isomaltose, isomaltotriose, and melibiose.

The observed fragment ions in both ion modes are summarized in Table 2. The low abundance of precursor ions disallowed getting MS^2 spectra of several deprotonated molecules. In these cases chloride adducts were used for fragmentation studies.

Cross-ring fragmentations of cation adducts, as well deprotonated glucooligosaccharides related to losses of 60, 90 and 120 Da have been attributed to neutral molecules $C_2H_4O_2$, $C_3H_6O_3$, and $C_4H_8O_4$ respectively [5,25–27]. The formation of the $[M-H-78]^-$ ion was the result of the subsequent dehydration of $[M-H-60]^-$ ion [5,27].

The predominant mechanism of fragmentation of cationized oligosaccharides involves a series of retro-aldol reactions occurring on the reducing end of the molecule, as elucidated in detail in ref. [22,25,27]. A similar pathway, retro-ene reaction, was suggested for a 90 Da loss [27]. The mechanisms proposed for the fragmentation of deprotonated molecules are similar to those of alkali metal adducts [18]. Molecular orbital calculation supported parallel formation of 60, 90, and 120 Da species for α-(1 → 6) linked glucose units [28].

The anions at *m*/*z* 221 obtained from deprotonated (1 → 4) and (1 → 6) glucose disaccharides by the direct loss of 120 Da in fact consisted of sugar moiety linked to glycolaldehyde. The structures of these ions were based on the comparison to synthetic standards [29]. The loss of $C_2H_4O_2$ including anomeric and adjacent carbon atom was confirmed with the ^{13}C-labeled lactose [18]. In the negative-ion mode, the proposed mechanism for the formation of several fragments of *N*-glycan mannose core corresponding to losses of 90 and 120 Da was reported by Harvey [15].

With the assignment of the specific product ion to α-(1 → 4), respective α-(1 → 6) linkages were supported by the set of experiments applied to oligosaccharides with a more complex structure. Since panose contains both α-(1 → 4) and α-(1 → 6) glycosidic bonds, it was a proper model for testing the sequencing abilities of ESI-IT-MS. Both MS and MS^2 spectra of sodium and chloride adducts and the deprotonated molecule are shown in Fig. 4. In the negative-ion mode mass spectra, the presence of an ion at *m*/*z* 425 (corresponding to neutral loss 78 Da) and the absence of an ion at *m*/*z* 413 was a diagnostic of an α-(1 → 4) structure (Fig. 4e and f). The second glycosidic bond, α-(1 → 6), was characterized by the presence of an ion at *m*/*z* 251 (neutral loss 90 Da; see Fig. 4f). This result corresponds to the fragmentation pathway starting from the reducing end of the panose molecule (for structure, see formula in

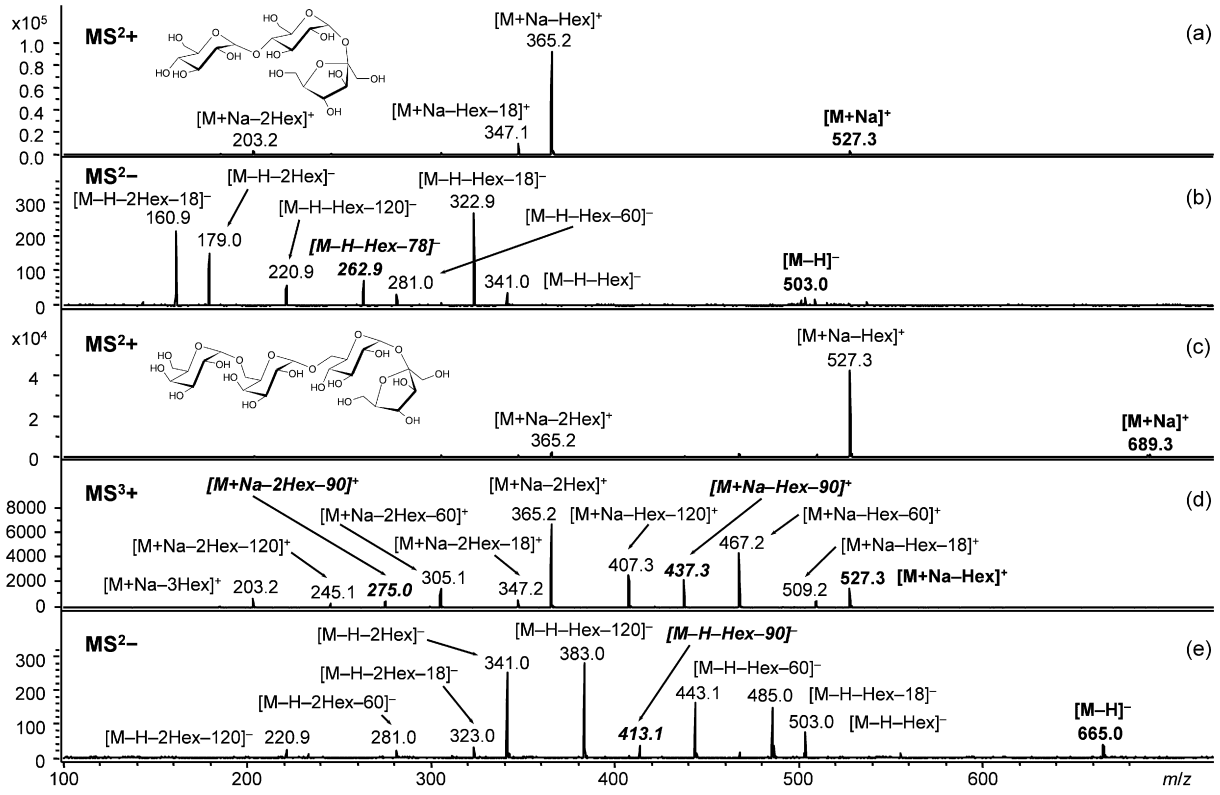

Fig. 5. ESI-MS^2 spectra of $[M+Na]^+$ (a) and $[M-H]^-$ ions (b) from erlose, and spectra of $[M+Na]^+$ (c) and $[M-H]^-$ ions (e) from stachyose. MS^3 spectrum of product ion $[M+Na-Hex]^+$ derived from stachyose (d). Precursor ions are in bold, diagnostic fragments are in bold italics.

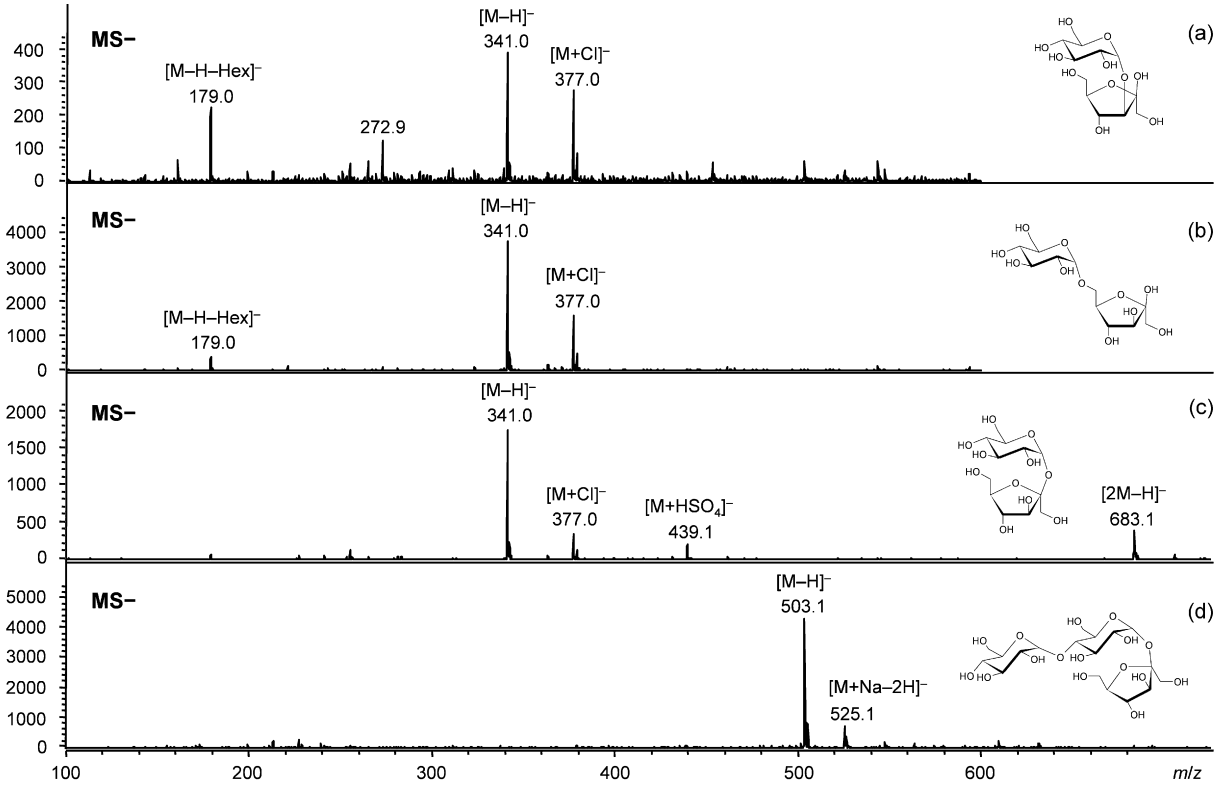

Fig. 6. Comparison of negative-ion mass spectra of turanose (a), palatinose (b), sucrose (c), and erlose (d).

Fig. 4). Similarly, the absence of an ion at m/z 437 in the product ion spectrum of $[M+Na]^+$ is consistent with α-(1 → 4) linkage between the residues at the reducing end (Fig. 4d). The ions observed at m/z 347 and 305, formed by loss of one glucose residue and water or 60 Da, did not allow a reliable attributing remaining linkage. Nevertheless, a desired $[M+Na-Hex-90]^+$ ion was found in the MS^3 spectra of ions at m/z 407, as well as 365, which also leads to the identification of panose (Fig. 4d). Whereas the differentiation between α-(1 → 4) and α-(1 → 6) linkages from the fragment spectrum of the sodium adduct is complicated, the fragment spectra of both the deprotonated molecule and the chloride adduct clearly show the differences in the specific fragmentation pattern.

Analogously, the fragmentation behavior of erlose and stachyose was studied. These nonreducing saccharides contain, in addition to starch-like moiety, the same disaccharide part, terminal sucrose unit. From the negative-ion MS^2 spectra of erlose and stachyose (Fig. 5b and e), it is evident that loss of the terminal fructose residue occurs [30,31]. It was followed by fragmentation of the remaining part of the saccharide, providing several types of product ions. The similar fragmentation patterns appeared for both oligosaccharides, with exception of ions at m/z 263 (for erlose) and 413 (for stachyose). The first ion, corresponding to $[M-H-Hex-78]^-$, can be used as a diagnostic indicator of α-(1 → 4) linkage, the second one (i.e., $[M-H-Hex-90]^-$) provides evidence for the presence of α-(1 → 6) linkage adjacent to the sucrose part. No cross-ring fragments in the mass range between $[M-H-Hex]^-$ and $[M-H]^-$ (precursor ion) were detected. Compared to the negative-ion mass spectra, the positive-ion product spectra produced fewer ion species. The spectrum of sodiated erlose was dominated by an ion at m/z 365 arising from a loss of a hexose unit. The ions at m/z 203, 305, and 347 were of low intensity. Sodiated stachyose underwent fragmentation consistent with that observed for erlose. To distinguish between α-(1 → 4) and α-(1 → 6) linkages, abundant ions were selected for MS^3 experiments. An MS^3 spectrum of $[M+Na-Hex]^+$ ion (m/z 527) derived from stachyose contained an abundant ion at m/z 437 corresponding to $[M+Na-Hex-90]^+$ (Fig. 5d). This observation allowed the assignment of α-(1 → 6) linkage. As expected, this specific fragment ion was not observed for erlose (m/z 365) that does not contain α-(1 → 6) linkage.

With reference to studied nonreducing saccharides (erlose, stachyose), the initial loss of a hexose is probably related to the release of terminal (α1 ↔ β2)Fru. The same result was obtained regarding sucrose. These observations indicate that nonreducing saccharides yield $[M-H]^-$ ions that are less susceptible to consecutive decomposition. Having only the ion adducts and the deprotonated molecules in mass spectra (Fig. 6c and d) they corroborated this suggestion. On the other hand, the reducing saccharides containing terminal fructose (e.g., turanose, palatinose) showed the fragment ions in their mass spectra (Fig. 6a and b). This phenomenon, as well preferential fragmentation of $[M-H]^-$ ions on glycosidic bond between glucose and fructose, can also facilitate the differentiation of reducing and nonreducing saccharides with a terminal fructose unit. The same conclusions were deduced from MALDI measurements of reducing and nonreducing saccharides [24].

4. Conclusions

The oligosaccharides containing Hex-α-(1 → 4)Hex and Hex-α-(1 → 6)Hex structural motifs examined in this study were readily amenable to analysis by negative-ion ESI-IT-MS. Tandem mass spectrometry permitted unambiguous differentiation of the α-(1 → 4) and α-(1 → 6) linkages using the presence of specific fragment ions. It seems that the method is particularly useful for identification of partially hydrolyzed starch oligosaccharides as well as for sequencing various oligosaccharides.

The MS^2 spectra obtained in the negative-ion mode enable identification of ions specific for both types of studied glycosidic linkages. On the other hand, the positive-ion mode, while more sensitive, gives no diagnostic ion for α-(1 → 4) linkage. Absence of a structural indicator plays a crucial role in the correct determination of glycosidic linkage following the first cleaved one. In these cases, some less abundant ions could not be detected and therefore the false linkage can be deduced. The advantage of the higher sensitivity of the positive-ion mode could be compensated by the addition of appropriate ammonium salts (e.g., NH_4Cl), which enhances ion signals in the negative-ion mode.

Oligosaccharides terminated with sucrose moiety showed $[M-H]^-$, $[M+Cl]^-$, respective $[M+Na]^+$ ions in mass spectra, which were usually accompanied by a small amount of ions related to in-source fragmentation. In the MS^2 spectra of mentioned precursor ions, characteristic ions attributed to the initial loss of fructose residue and ions corresponding to the subsequent fragmentation of $[M-H-Fru]^-$ or $[M+Na-Fru]^+$ product ions. Both characteristic features of behavior make possible discrimination between the common types of reducing and nonreducing oligosaccharides.

Acknowledgements

This work was supported by the Institutional Research Plan AV0Z40310501 and by the Project no. 2B06037 from the Ministry of Education, Youth and Sports, Czech Republic.

References

[1] S. Ball, H.P. Guan, M. James, A. Myers, P. Keeling, G. Mouille, A. Buléon, P. Colonna, J. Preiss, From glycogen to amylopectin: a model for the biogenesis of the plant starch granule, Cell 86 (1996) 349–352.
[2] A. Buléon, P. Colonna, V. Planchot, S. Ball, Starch granules: structure and biosynthesis, Int. J. Biol. Macromol. 23 (1998) 85–112.
[3] D.J. Manners, The enzymic degradation of starches, in: J.M.V. Blanshard, J.R. Mitchell (Eds.), Polysaccharides in Food, Butterworths, London, 1979, pp. 75–92.
[4] M. Bachmann, P. Matile, F. Keller, Metabolism of the raffinose family oligosaccharides in leaves of Ajuga reptans L. (Cold acclimation, translocation, and sink to source transition: discovery of chain elongation enzyme), Plant Physiol. 105 (1994) 1335–1345.
[5] D. Garozzo, M. Giuffrida, G. Impallomeni, A. Ballistreri, G. Montaudo, Determination of linkage position and identification of the reducing end in linear oligosaccharides by negative ion fast atom bombardment mass spectrometry, Anal. Chem. 62 (1990) 279–286.
[6] D.J. Harvey, Matrix-assisted laser desorption/ionization mass spectrometry of carbohydrates and glycoconjugates, Int. J. Mass Spectrom. 226 (2003) 1–35.
[7] J. Zaia, Mass spectrometry of oligosaccharides, Mass Spectrom. Rev. 23 (2004) 161–227.
[8] D.J. Harvey, Structural determination of N-linked glycans by matrix-assisted laser desorption/ionization and electrospray ionization mass spectrometry, Proteomics 5 (2005) 1774–1786.
[9] D.J. Harvey, Fragmentation of negative ions from carbohydrates: Part 1. Use of nitrate and other anionic adducts for the production of negative ion electrospray spectra from N-linked carbohydrates, J. Am. Soc. Mass Spectrom. 16 (2005) 622–630.
[10] R. Čmelík, M. Štikarovská, J. Chmelík, Different behavior of dextrans in positive-ion and negative-ion mass spectrometry, J. Mass Spectrom. 39 (2004) 1467–1473.
[11] Y. Cai, Y. Jiang, R.B. Cole, Anionic adducts of oligosaccharides by matrix-assisted laser desorption/ionization time-of-flight mass spectrometry, Anal. Chem. 75 (2003) 1638–1644.
[12] V.N. Reinhold, B.B. Reinhold, C.E. Costello, Carbohydrate molecular weight profiling, sequence, linkage, and branching data: ES-MS and CID, Anal. Chem. 67 (1995) 1772–1784.
[13] D.J. Harvey, R.H. Bateman, R.S. Bordoli, R. Tyldesley, Ionisation and fragmentation of complex glycans with a quadrupole time-of-flight mass spectrometer fitted with a matrix-assisted laser desorption/ionisation ion source, Rapid Commun. Mass Spectrom. 14 (2000) 2135–2142.
[14] Y. Jiang, R.B. Cole, Oligosaccharide analysis using anion attachment in negative mode electrospray mass spectrometry, J. Am. Soc. Mass Spectrom. 16 (2005) 60–70.

[15] D.J. Harvey, Fragmentation of negative ions from carbohydrates: Part 2. Fragmentation of high-mannose N-linked glycans, J. Am. Soc. Mass Spectrom. 16 (2005) 631–646.
[16] C.H. Friedl, G. Lochnit, R. Geyer, M. Karas, U. Bahr, Structural elucidation of zwitterionic sugar cores from glycosphingolipids by nanoelectrospray ionization–ion-trap mass spectrometry, Anal. Biochem. 284 (2000) 279–287.
[17] S. Pasanen, J. Jänis, P. Vainiotalo, Cello-, malto- and xylooligosaccharide fragmentation by collision-induced dissociation using QIT and FT-ICR mass spectrometry: a systematic study, Int. J. Mass Spectrom. 263 (2007) 22–29.
[18] J.A. Carroll, L. Ngoka, C.G. Beggs, C.B. Lebrilla, Liquid secondary ion mass spectrometry/fourier transform mass spectrometry of oligosaccharide anions, Anal. Chem. 65 (1993) 1582–1587.
[19] Y. Mechref, M.V. Novotny, Structural characterization of oligosaccharides using Maldi-TOF/TOF tandem mass spectrometry, Anal. Chem. 75 (2003) 4895–4903.
[20] A.H. Que, M.V. Novotny, Structural characterization of neutral oligosaccharide mixtures through a combination of capillary electrochromatography and ion trap tandem mass spectrometry, Anal. Bioanal. Chem. 375 (2003) 599–608.
[21] J. Simoes, P. Domingues, A. Reis, F.M. Nunes, M.A. Coimbra, M.R.M. Domingues, Identification of anomeric configuration of underivatized reducing glucopyranosyl-glucose disaccharides by tandem mass spectrometry and multivariate analysis, Anal. Chem. 79 (2007) 5896–5905.
[22] Z. Zhou, S. Ogden, J.A. Leary, Linkage position determination in oligosaccharides: mass spectrometry (MS/MS) study of lithium-cationized carbohydrates, J. Org. Chem. 55 (1990) 5444–5446.
[23] N. Penna, S. Capellacci, F. Ricci, M. Giorgi, A. Penna, G. Famiglini, E. Pierini, H. Trufelli, A. Cappiello, Study on the maltooligosaccharide composition of mucilage samples collected along the northern Adriatic coast, Carbohydr. Res. 344 (2009) 120–126.
[24] M. Laštovičková, J. Chmelík, Simple and fast method for recognition of reducing and nonreducing neutral carbohydrates by matrix-assisted laser desorption/ionization time-of-flight mass spectrometry, J. Agric. Food Chem. 54 (2006) 5092–5097.
[25] G.E. Hofmeister, Z. Zhou, J.A. Leary, Linkage position determination in lithium-cationized disaccharides: tandem mass spectrometry and semiempirical calculations, J. Am. Chem. Soc. 113 (1991) 5964–5970.
[26] M.R. Asam, G.L. Glish, Tandem mass spectrometry of alkali cationized polysaccharides in a quadrupole ion trap, J. Am. Soc. Mass Spectrom. 8 (1997) 987–995.
[27] B. Spengler, J.W. Dolce, R.J. Cotter, Infrared laser desorption mass spectrometry of oligosaccharides: fragmentation mechanisms and isomer analysis, Anal. Chem. 62 (1990) 1731–1737.
[28] J.A. Carroll, D. Willard, C.B. Lebrilla, Energetics of cross-ring cleavages and their relevance to the linkage determination of oligosaccharides, Anal. Chim. Acta 307 (1995) 431–447.
[29] T.T. Fang, J. Zirrolli, B. Bendiak, Differentiation of the anomeric configuration and ring form of glucosyl-glycolaldehyde anions in the gas phase by mass spectrometry: isomeric discrimination between m/z 221 anions derived from disaccharides and chemical synthesis of m/z 221 standards, Carbohydr. Res. 342 (2007) 217–235.
[30] R.E. March, C.J. Stadey, A tandem mass spectrometric study of saccharides at high mass resolution, Rapid Commun. Mass Spectrom. 19 (2005) 805–812.
[31] J. Zhu, R.B. Cole, Ranking of gas-phase acidities and chloride affinities of monosaccharides and linkage specificity in collision-induced decompositions of negative ion electrospray-generated chloride adducts of oligosaccharides, J. Am. Soc. Mass Spectrom. 12 (2001) 1193–1204.